

# Swelling of two-dimensional polymer rings by trapped particles

Emir Haleva and Haim Diamant

School of Chemistry, Raymond & Beverly Sackler Faculty of Exact Sciences, Tel Aviv University, Tel Aviv 69978, Israel

Received: date / Revised version: date

**Abstract.** The mean area of a two-dimensional Gaussian ring of  $N$  monomers is known to diverge when the ring is subject to a critical pressure differential,  $p_c \sim N^{-1}$ . In a recent publication [Eur. Phys. J. E **19**, 461 (2006)] we have shown that for an inextensible freely jointed ring this divergence turns into a second-order transition from a crumpled state, where the mean area scales as  $\langle A \rangle \sim N$ , to a smooth state with  $\langle A \rangle \sim N^2$ . In the current work we extend these two models to the case where the swelling of the ring is caused by trapped ideal-gas particles. The Gaussian model is solved exactly, and the freely jointed one is treated using a Flory argument, mean-field theory, and Monte Carlo simulations. For a fixed number  $Q$  of trapped particles the criticality disappears in both models through an unusual mechanism, arising from the absence of an area constraint. In the Gaussian case the ring swells to such a mean area,  $\langle A \rangle \sim NQ$ , that the pressure exerted by the particles is at  $p_c$  for any  $Q$ . In the freely jointed model the mean area is such that the particle pressure is always higher than  $p_c$ , and  $\langle A \rangle$  consequently follows a single scaling law,  $\langle A \rangle \sim N^2 f(Q/N)$ , for any  $Q$ . By contrast, when the particles are in contact with a reservoir of fixed chemical potential, the criticality is retained. Thus, the two ensembles are manifestly inequivalent in these systems.

**PACS.** 36.20.Ey Macromolecules and polymer molecules: Conformation (statistics and dynamics) – 64.60.Cn Order-disorder transformations; statistical mechanics of model systems – 61.25.Hq Swelling of polymers

## 1 Introduction

Polymer rings confined to two dimensions (2D) have been the subject of several theoretical works [1, 2, 3, 4, 5, 6, 7, 8, 9, 10, 11, 12, 13, 14], in part as highly idealized models for membrane vesicles. The statistics of 2D chains have been studied also experimentally, using polymers adsorbed at liquid interfaces [15, 16] or membranes [17], as well as vibrated granular chains [18] and rings [19]. In those experimental systems both random-walk and self-avoiding-walk statistics were observed.

Pressurized 2D rings were theoretically investigated in a number of works [6, 7, 8, 9, 10, 11, 12, 13, 14]. In the Rudnick-Gaspari model [9, 10, 11] the ring is represented by a closed Gaussian chain of  $N$  springs subject to an inflating pressure differential  $p$ . This model yields a divergent mean area at a critical pressure,  $p_c \sim N^{-1}$ . Recently we have demonstrated that the inclusion of chain inextensibility (*i.e.*, considering a freely jointed chain rather than a Gaussian one) turns this divergence into a second-order smoothening transition [14]. For  $p < p_c$  the ring is in a crumpled, random-walk state with the mean area scaling as  $\langle A \rangle \sim N f^<(pN)$ , whereas for  $p > p_c$  the ring is smooth with  $\langle A \rangle \sim N^2 f^>(pN)$ .

In many practical cases a pressure difference across a closed surface is achieved osmotically through a concentration difference, *e.g.*, by trapping particles inside the

envelope. In the current study we extend the models of pressurized Gaussian and freely jointed 2D rings to the case where the swelling is caused by a trapped ideal gas of particles. We examine both the canonical and grand-canonical ensembles, in which the particle number  $Q$  or the particle fugacity  $\gamma$  are fixed, respectively.

The model is defined in the following section. In Section 3 we derive exact results for a Gaussian ring swollen by trapped particles. We then treat the swelling of a freely jointed ring in Section 4 by employing a Flory argument, mean-field calculation and Monte Carlo simulations. In addition, we derive exact asymptotes for the large-swellings regime. Finally, the results are discussed in Section 5.

## 2 Model

We model a 2D polymer ring as a closed ideal chain of  $N$  monomers and no bending rigidity. The ring encapsulates an ideal gas of particles. We shall consider separately the two cases of a Gaussian and a freely jointed chain. The unperturbed monomer-monomer link length is taken as the unit length,  $l \equiv 1$ . For a freely jointed chain this length remains fixed under swelling. For a Gaussian chain, however, the link length has a statistical distribution that varies with swelling;  $l$  is then defined as the unperturbed root-mean-square link length.

In a canonical ensemble, where the number  $Q$  of particles is fixed, the partition function is given, up to a constant prefactor, by

$$Z(N, Q) = \int_0^\infty dA P_0(N, A) A^Q / Q!, \quad (1)$$

where  $A$  is the area bounded by the ring, and  $P_0(N, A)$  is the probability distribution function of the area for an unpressurized  $N$ -monomer ring (for either a Gaussian or a freely jointed chain). The mean area of the ring is given by

$$\langle A(N, Q) \rangle = (Q + 1) Z(N, Q + 1) / Z(N, Q). \quad (2)$$

In a grand-canonical ensemble, where the particles are in contact with a reservoir of fixed fugacity  $\gamma$ , we use equation (1) to write the grand partition function as

$$\mathcal{Z}(N, \gamma) = \sum_{Q=0}^{\infty} Z(N, Q) \gamma^Q = \int_0^\infty dA P_0(N, A) e^{\gamma A}. \quad (3)$$

The mean area in this ensemble is given, therefore, by

$$\langle A(N, \gamma) \rangle = \partial \ln \mathcal{Z} / \partial \gamma, \quad (4)$$

and the mean particle number by

$$\langle Q(N, \gamma) \rangle = \partial \ln \mathcal{Z} / \partial \ln \gamma = \gamma \langle A \rangle. \quad (5)$$

Thus, the mean particle density,  $c = \langle Q \rangle / \langle A \rangle$ , is equal to the fugacity  $\gamma$ , as it should for an ideal gas.

The correlation between fluctuations in particle number and in the ring area is characterized by the following covariance,

$$C_{QA}(N, \gamma) = \frac{\langle QA \rangle - \langle Q \rangle \langle A \rangle}{\langle Q \rangle \langle A \rangle}. \quad (6)$$

From equation (3) we find

$$\langle QA \rangle = \frac{1}{\mathcal{Z}} \frac{\partial^2 \mathcal{Z}}{\partial (\ln \gamma) \partial \gamma} = \gamma \langle A^2 \rangle, \quad (7)$$

which, combined with equation (5), yields

$$C_{QA}(N, \gamma) = \frac{\langle \Delta A^2 \rangle}{\langle A \rangle^2}, \quad (8)$$

where  $\langle \Delta A^2 \rangle = \langle A^2 \rangle - \langle A \rangle^2$  is the mean-square area fluctuation. Hence, interestingly, the cross-correlation of  $Q$  and  $A$  is identical to the relative mean-square fluctuation in the ring area.

Our model system consists of two subsystems — particles and ring monomers — which may have different relaxation times. We note, however, that in equations (1) and (3) all configurations of both subsystems are traced over. Hence, the equilibrium properties studied in this paper are unaffected by such time-scale differences.

Several complications related to the definition of the ring area in the model should be mentioned. In principle

the  $A$  appearing in equation (1) should be the *geometrical* area  $A_g$  of the ring, since it is  $A_g$  that determines the translational entropy of the particles. As in previous works [9, 10, 11, 14], however, we are technically bound to use the *algebraic* area  $A$  instead, *i.e.*, the area obtained from an integral over the ring contour. This area may contain both positive and negative contributions,  $A_+$  and  $A_-$ . In an unperturbed ring positive and negative areas are equally favorable, and the mean algebraic area then vanishes. (The algebraic area may also “count” a certain geometrical-area contribution more than once due to chain winding.) On the one hand, particle entropy forces us to use only the positive-area part of  $P_0$  (hence the integration from 0 to  $\infty$  in equation (1)). Consequently, the mean algebraic area of an unperturbed ring,  $\langle A \rangle$ , does not vanish. This is the definition used in the analytical parts of this work. In the simulations, on the other hand, we follow changes in the actual algebraic area of the ring, allowing the total area to become negative. Thus, in the numerical parts of this work  $\langle A \rangle$  of an unperturbed ring does vanish. In addition, the simulated particles are placed only inside positive parts of the ring area, *i.e.*, their entropy-relevant area is  $A_+ \neq A$ . Finally, in equation (3) one notices a direct analogy between the problem of fixed particle fugacity studied here and that of an empty ring subject to a fixed pressure, which was studied in [9, 14]. The mapping is not exact, however, since in the current case  $A$  is restricted to positive values, whereas in [9, 14] it was not. All these subtleties are significant only in the weak-swelling regime of small areas. As the inner pressure exerted by the particles increases, the distinction between the various area definitions becomes negligible and does not affect our main results as will be demonstrated below, as will be demonstrated below.

### 3 Gaussian Ring

In this section we consider a 2D Gaussian ring swollen by trapped particles, for which exact results can be derived. The chain consists of a set of  $N$  springs with fixed spring constant,  $\lambda = 1$ , in units of  $k_B T / l^2$  (to yield an unperturbed root-mean-square spring length of  $l = 1$ ). For the sake of the following sections, in which the spring constant is allowed to change, we keep the results dependent on  $\lambda$  without substituting  $\lambda = 1$ .

#### 3.1 Canonical Ensemble

The probability distribution function of the algebraic area for a 2D Gaussian ring was calculated by Khandekar and Wiegel [2, 3],<sup>1</sup>

$$P_0^G(N, A) = \frac{1}{\lambda^N} \frac{2\pi\lambda}{N \cosh^2(2\pi\lambda A/N)}. \quad (9)$$

<sup>1</sup> Equation (9) differs from the original Khandekar-Wiegel expression by a factor of 2, since the particle translational entropy in the current model restricts our analysis to positive areas (Eq. (1)).

Substituting equation (9) in equation (1), we obtain the exact partition function,

$$Z^G(N, Q) = \frac{2}{\lambda^N} \left( \frac{N}{4\pi\lambda} \right)^Q (1 - 2^{1-Q}) \zeta(Q), \quad (10)$$

where  $\zeta$  is the Riemann zeta function. The mean area is then given, according to equation (2), by

$$\langle A^G(N, Q) \rangle = \frac{N(Q+1)}{4\pi\lambda} \frac{1 - 2^{-Q}}{1 - 2^{1-Q}} \frac{\zeta(Q+1)}{\zeta(Q)}, \quad (11)$$

which turns, in the limit of large  $Q$ , to

$$\langle A^G(N, Q \gg 1) \rangle = NQ/(4\pi\lambda). \quad (12)$$

In the current case of fixed  $\lambda$ , we thus get that the ring swells gradually (linearly) with  $Q$ . This is qualitatively different from the Rudnick-Gaspari result for the swelling as a function of fixed pressure [9,10,11], where the mean area diverges at a finite critical pressure,  $p_c = 4\pi/N$  (in units of  $k_B T/l^2$ ). The ability of the Gaussian ring to swell indefinitely stems, as in the Rudnick-Gaspari model, from its extensibility.

Since the mean area is proportional to  $Q$ , we obtain in this ensemble the peculiar result that the particle density is independent of particle number,

$$c^G(N) = Q/\langle A^G \rangle = 4\pi\lambda/N. \quad (13)$$

The same holds for the particle fugacity,

$$\gamma^G(N) = \exp(-\partial \ln Z^G / \partial Q) = 4\pi\lambda/N, \quad (14)$$

which is equal to the density of equation (13), as expected for an ideal gas. The mean pressure of the gas, in our dimensionless units, is  $p = c = 4\pi/N$ . (Recall that  $\lambda = 1$ .) Thus, for any  $Q$  the ring swells to such an extent that the pressure exerted on it by the gas is always at the Rudnick-Gaspari  $p_c$ , yet without the associated criticality.

### 3.2 Grand-Canonical Ensemble

The grand partition function is obtained from equations (3) and (9) as

$$\mathcal{Z}^G(N, \gamma) = \frac{1}{\lambda^{N+1}} [-\lambda + \psi(-x) - \psi(1/2 - x)], \quad (15)$$

where  $x \equiv \gamma N/(8\pi\lambda)$ , and  $\psi$  is the digamma function (the logarithmic derivative of the gamma function). The mean area is calculated according to equation (4), yielding

$$\langle A^G(N, \gamma) \rangle = \frac{1}{\lambda^N \mathcal{Z}^G} \frac{N}{4\pi\lambda} \{ \psi(-x) - \psi(1/2 - x) - x [\psi'(-x) - \psi'(1/2 - x)] \}, \quad (16)$$

where prime denotes a first derivative. The mean number of trapped particles, according to equation (5), is simply given by  $\langle Q^G \rangle = \gamma \langle A^G \rangle$ .

The digamma function and its derivative diverge for small arguments as  $\psi(x) \simeq -x^{-1}$  and  $\psi'(x) \simeq x^{-2}$ , respectively. Thus, the expressions for  $\mathcal{Z}^G$ ,  $\langle A^G \rangle$ , and  $\langle Q^G \rangle$  diverge at a critical fugacity (with  $\lambda = 1$ ),

$$\gamma_c = 4\pi/N. \quad (17)$$

Since for the ideal gas  $p = c = \gamma$ , this divergence is analogous to that of the Rudnick-Gaspari model at  $p_c = 4\pi/N$ .

## 4 Freely Jointed Ring

We now turn to the case of a freely jointed chain, *i.e.*, an inextensible ring whose link lengths are fixed.

### 4.1 Canonical Ensemble

#### 4.1.1 Flory Argument

We begin by examining a simple Flory argument, following the lines of [14]. The free energy of the ring (in units of  $k_B T$ ) is expressed as a function of  $R$ , the radius of the statistical cloud of monomers (*i.e.*, the mean radius of gyration). We divide it into three terms,

$$F(R, Q) = F_{\text{el}} + F_{\text{inext}} + F_{\text{en}}, \quad (18)$$

$$F_{\text{el}} \sim R^2/N, \quad F_{\text{inext}} \sim R^4/N^3, \quad F_{\text{en}} \sim Q[\ln(Q/R^2) - 1].$$

The first term is the usual entropic-spring free energy of a Gaussian chain [20]. The second is the leading non-Gaussian correction due to inextensibility (see App. A of [14]). The last term comes from the translational entropy of the ideal gas, where the mean area of the ring is taken proportional to  $R^2$  [4,5].

Unlike the case of fixed pressure [14], the free energy of equation (18) exhibits no phase transition with increasing  $Q$ . Upon minimization with respect to  $R$  we get the following scaling law:

$$R^2 \sim N^2 f(Q/N), \quad (19)$$

which, despite the crudeness of the Flory argument, turns out to be correct, as demonstrated below.

#### 4.1.2 Mean-Field Approximation

We proceed to study the freely jointed model by relaxing the strict constraints of fixed link lengths into harmonic potentials. This kind of approximation, used in several previous polymer theories [21,22,23,14], is equivalent to a mean-field assumption [22]. The calculation is identical to that for a Gaussian chain (Sec. 3), yet the spring constant  $\lambda$  is not fixed but determined self-consistently to maintain the root-mean-square link length equal to  $l = 1$ .

To impose the relaxed inextensibility constraint we differentiate  $Z^G$  with respect to  $\lambda$  to get the mean-square link length, and then set it to 1,

$$-N^{-1} \partial \ln Z^G / \partial \lambda = (1 + \hat{Q})/\lambda = 1, \quad (20)$$

where  $\hat{Q} \equiv Q/N$  is the rescaled particle number. For  $\hat{Q} \rightarrow 0$  we get  $\lambda = 1$ , as expected, but as the number of trapped particles increases, the springs get stiffer according to

$$\lambda = 1 + \hat{Q}. \quad (21)$$

This value is substituted in equation (12) to obtain

$$\langle A^{\text{FJ}}(N, \hat{Q}) \rangle = A_{\max} \hat{Q} / (\hat{Q} + 1). \quad (22)$$

As  $\hat{Q} \rightarrow \infty$  the mean area appropriately tends to its maximum value,  $A_{\max} = N^2/(4\pi)$ , which is the area of a circle with perimeter  $N$ . Equation (22) shows that the swelling of the ring with increasing  $Q$  is gradual, without any phase transition.

The particle density is given by

$$c^{\text{FJ}}(N, \hat{Q}) = Q / \langle A^{\text{FJ}} \rangle = 4\pi(\hat{Q} + 1)/N. \quad (23)$$

The fugacity is found from equations (14) and (21) as

$$\gamma^{\text{FJ}}(N, \hat{Q}) = 4\pi(\hat{Q} + 1)/N, \quad (24)$$

which is equal to  $c^{\text{FJ}}$ , as it should for an ideal gas. The exerted pressure is  $p = \gamma = (4\pi/N)(\hat{Q} + 1)$ , which is larger than  $p_c = 4\pi/N$  for any  $Q$ .

#### 4.1.3 Exact Asymptote for Strong Swelling

In the limit of large particle number,  $\hat{Q} \gg 1$ , the partition function can be calculated exactly. In this limit the chain is highly swollen and its statistics is governed by large-area conformations. Thus, to apply equation (1), we merely need to know how the area probability distribution function for a 2D freely jointed ring,  $P_0^{\text{FJ}}(N, A)$ , decays to zero as  $A$  approaches  $A_{\max}$ . This calculation is presented in Appendix A. The result is

$$P_0^{\text{FJ}}(N, A \lesssim A_{\max}) \sim (A_{\max} - A)^{N/2}. \quad (25)$$

Substituting equation (25) in equation (1), we get

$$Z^{\text{FJ}}(N, Q \gg N) = (A_{\max})^{Q+N/2} \frac{\Gamma(1 + N/2)}{\Gamma(1 + N/2 + Q)}, \quad (26)$$

where  $\Gamma$  is the gamma function. The mean area is then obtained from equation (2) as

$$\langle A^{\text{FJ}}(N, \hat{Q} \gg 1) \rangle \simeq A_{\max} \frac{\hat{Q}}{\hat{Q} + 1/2} \simeq A_{\max} \left(1 - \frac{1}{2\hat{Q}}\right). \quad (27)$$

Thus, the exact approach of the mean area to its maximum value differs from the mean-field result, equation (22), by a factor of 1/2.

#### 4.1.4 Monte Carlo Simulations

We performed Monte Carlo simulations to obtain the mean area  $\langle A \rangle$  of a freely jointed ring as a function of the number  $Q$  of trapped ideal-gas particles for various ring sizes  $N$ . The algorithm combines an off-lattice scheme for the polymer, as was used in [14], with a lattice model for the particles. The simulated system is schematically shown in Figure 1. The ring is represented by a polygon of  $N$  equal edges of length  $l = 1$ . The 2D coordinates of the vertices take continuous values. The coordinates of the particles are defined on a 2D square lattice with lattice constant of either  $l$  or  $l/5$ , depending on the required precision.

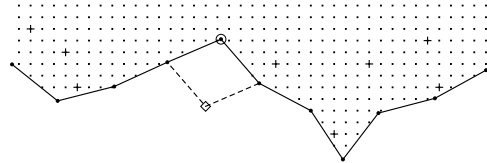


**Fig. 1.** Schematic view of a section of the simulated system. Point particles (marked by '+') are located on lattice sites confined inside the ring. On each step each particle is moved to a randomly chosen neighboring site. In the second part of the step a single randomly chosen chain vertex (marked by a circle) is moved to the only other position (marked by a diamond) that maintains the lengths of the two links attached to it.

The initial configuration is a fully stretched, regular polygon of purely positive algebraic area,  $A = A_+$ . During the simulation we keep track of positive and negative contributions to  $A$  and place particles only on lattice sites belonging to  $A_+$ . Each step of the simulation is composed of two actions. In the first, each particle is moved to a randomly chosen juxtaposed lattice site, unless this site is outside the positive-area part of the polygon. In the second action, a randomly chosen chain vertex is moved to the only other position that satisfies the edge-length constraint (see Fig. 1). This action is automatically rejected if it makes a particle leave the positive-area part of the ring. These dynamics involve  $O(Q)$  operations per step. The number of operations required for equilibration is  $O(N^3Q)$ , limiting our investigation to  $N \lesssim 500$ . The simulations were performed for  $N$  between 50 and 400 and  $Q$  between 0 and  $4N$ .

Figure 2 shows the simulation results for the mean area (scaled by  $A_{\max} \sim N^2$ ) as a function of the rescaled particle number  $\hat{Q} = Q/N$ . All data for different values of  $N$  collapse onto a single universal curve, in accord with the scaling law obtained from the Flory argument and mean-field calculation (Eqs. (19) and (22)). Yet, only for small  $\hat{Q}$

does this curve coincide with the mean-field scaling function. For such small  $\hat{Q}$  it coincides also with the Gaussian result, (Eq. (12) with  $\lambda = 1$ ).

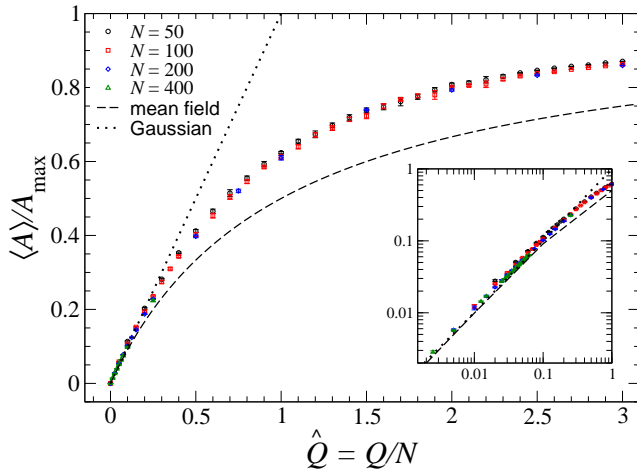


**Fig. 2.** (Color online) Mean area of a freely jointed ring, scaled by  $A_{\max} \sim N^2$ , as a function of the rescaled number of particles. Monte Carlo simulation results for various values of  $N$  are represented by symbols with error bars. The dashed line shows the mean-field result (Eq. (22)). The result for a Gaussian ring (Eq. (12)) is given for reference (dotted line). The inset focuses on the small  $\hat{Q}$  region using a logarithmic scale.

To confirm the highly swollen behavior derived in Section 4.1.3 we simulated rings of  $N = 50$  with  $Q$  between 0 and  $50N$ . The results are presented in Figure 3, showing good agreement for large  $\hat{Q}$  with the exact asymptote, equation (27).

## 4.2 Grand-Canonical Ensemble

### 4.2.1 Flory Argument

To account for contact of the particles with a reservoir of fixed fugacity  $\gamma$  we add a  $-Q \ln \gamma$  term to the Flory free energy, equation (18). Minimization with respect to  $Q$  yields the following grand potential:

$$\mathcal{F}(R, \gamma) = F_{\text{el}} + F_{\text{inext}} + F_{\text{res}}, \quad (28)$$

$$F_{\text{el}} \sim R^2/N, \quad F_{\text{inext}} \sim R^4/N^3, \quad F_{\text{res}} \sim -\gamma R^2.$$

This Landau-like free energy has a second-order phase transition at  $\gamma_c \sim N^{-1}$ , similar to the one obtained for fixed pressure in [14]. For  $\gamma < \gamma_c$   $F_{\text{inext}}$  is negligible, and  $R$  has a Gaussian distribution with  $\langle R^2 \rangle \sim N(1 - \gamma/\gamma_c)^{-1}$ . For  $\gamma > \gamma_c$  we have  $R^2 \sim N^2(\gamma/\gamma_c - 1)$ .

### 4.2.2 Mean-Field Approximation

As in section 4.1.2 we apply a relaxed inextensibility constraint by determining the spring constant  $\lambda$  so that the

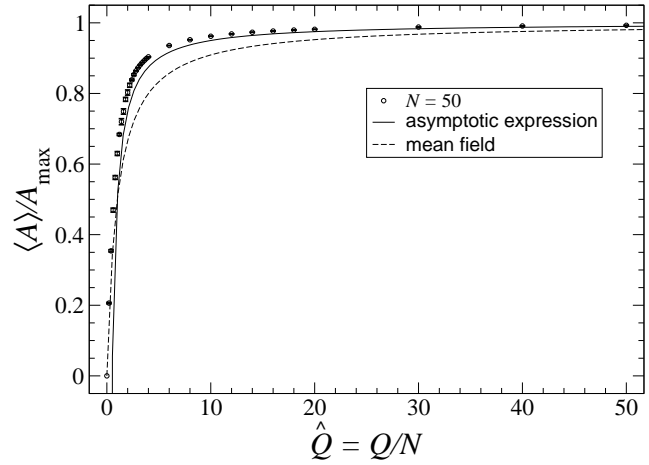


**Fig. 3.** Mean area of a freely jointed ring, scaled by  $A_{\max}$ , as a function of the rescaled particle number, as obtained by Monte Carlo simulations for  $N = 50$  (symbols with error bars). The solid line shows the exact asymptote for a highly swollen ring (Eq. (27)). The dashed line presents the mean-field result (Eq. (22)).

root-mean-square link length should be  $l = 1$ . In the current grand-canonical case this is done by differentiating  $\mathcal{Z}^G$  of equation (15) with respect to  $\lambda$ ,

$$\begin{aligned} & -N^{-1} \partial \ln \mathcal{Z}^G / \partial \lambda \\ &= \frac{1}{\lambda} + \frac{2}{\lambda^{N+1} N \mathcal{Z}^G} x \{ \psi(-x) - \psi(1/2 - x) \\ & \quad - x [\psi'(-x) - \psi'(1/2 - x)] \} = 1, \end{aligned} \quad (29)$$

thus obtaining a transcendental equation for  $\lambda(\gamma, N)$ . Equation (29) can be combined with equation (16) to get a simpler expression for  $\langle A \rangle$  as a function of  $\lambda$ ,

$$\langle A^{\text{FJ}}(N, \gamma, \lambda) \rangle = N(\lambda - 1)/\gamma. \quad (30)$$

Numerical solution of equation (29) for  $\lambda$  and substitution of the result in equation (30) yield the mean area as a function of  $\gamma$  and  $N$ .

We can get a good approximation for  $\lambda(\gamma, N)$  by substituting for the diverging terms in equation (29)  $\psi(x) \simeq -x^{-1}$  and  $\psi'(x) \simeq x^{-2}$ . This gives

$$\lambda(\hat{\gamma}, N \gg 1) \simeq \frac{\hat{\gamma} + 1 + \frac{1}{N} + \sqrt{(\hat{\gamma} - 1)^2 + \frac{2}{N}(\hat{\gamma} + 1) + \frac{1}{N^2}}}{2}, \quad (31)$$

where  $\hat{\gamma} \equiv \gamma N/(4\pi)$  is the rescaled fugacity. This result for  $\lambda$  is the same as the one obtained for fixed pressure  $p$  [14] with  $p = \gamma$ . In the thermodynamic limit, defined here as  $N \rightarrow \infty$  and  $\gamma \rightarrow 0$  such that  $\hat{\gamma}$  is finite, equation (31) reduces to the continuous but nonanalytic function,

$$\lambda(\hat{\gamma}, N \rightarrow \infty) = \begin{cases} 1 & \hat{\gamma} < 1 \\ \hat{\gamma} & \hat{\gamma} > 1. \end{cases} \quad (32)$$

Substituting equation (31) in equation (30) yields an approximate expression for  $\langle A \rangle$  as a function of  $\hat{\gamma}$  and  $N$ ,

$$\langle A^{\text{FJ}}(\hat{\gamma} \ll 1, N \gg 1) \rangle \simeq \frac{N^2 \hat{\gamma} - 1 + \frac{1}{N} + \sqrt{(\hat{\gamma} - 1)^2 + \frac{2}{N}(\hat{\gamma} + 1) + \frac{1}{N^2}}}{4\pi \frac{2\hat{\gamma}}{N}}, \quad (33)$$

which in the thermodynamic limit becomes

$$\langle A^{\text{FJ}} \rangle = \begin{cases} \frac{N}{4\pi} \frac{1}{\hat{\gamma}(1-\hat{\gamma})} \xrightarrow{\hat{\gamma} \rightarrow 1^-} \frac{N}{4\pi} \frac{1}{1-\hat{\gamma}} & 1-\hat{\gamma} \gg N^{-1/2} \\ \frac{N^3/2}{4\pi} & |\hat{\gamma} - 1| \ll N^{-1/2} \\ \frac{N^2}{4\pi} \frac{\hat{\gamma}-1}{\hat{\gamma}} \xrightarrow{\hat{\gamma} \rightarrow 1^+} \frac{N^2}{4\pi}(\hat{\gamma}-1) & \hat{\gamma} - 1 \gg N^{-1/2}, \end{cases} \quad (34)$$

thus exhibiting a continuous phase transition at  $\hat{\gamma}_c = 1$ , analogous to the one found for fixed pressure (Eq. (16) in [14]). As shown in equation (5), the mean number of trapped particles is given by  $\langle Q^{\text{FJ}} \rangle = \gamma \langle A^{\text{FJ}} \rangle$  and, therefore, undergoes the same transition at  $\hat{\gamma}_c$ .

#### 4.2.3 Exact Asymptote for Strong Swelling

As demonstrated above, and also confirmed by simulations in the next section, fixing the fugacity in the grand-canonical ensemble is analogous to fixing the pressure in an empty ring. Thus, to get the asymptotic swelling at high fugacity we can readily use the exact asymptote for high pressure derived in [14] and replace  $p \rightarrow \gamma$ . This yields

$$\langle A(\hat{\gamma} \gg 1, N) \rangle \simeq A_{\max} \frac{I_1(\hat{\gamma})}{I_0(\hat{\gamma})} \simeq A_{\max} \left(1 - \frac{1}{2\hat{\gamma}}\right), \quad (35)$$

where  $I_n$  are modified Bessel functions of the first kind.

#### 4.2.4 Monte Carlo Simulations

We performed grand-canonical Monte Carlo simulations to check the results of the preceding sections. To each step of the algorithm described in section 4.1.4 a third action is added as follows. Either a randomly chosen particle is removed with probability  $Q/(\gamma A_+)$ , or a particle is added to a randomly chosen site within the positive-area part of the ring with probability  $\gamma A_+/(Q + 1)$ .

Figure 4 shows simulation results for different values of  $N$  in the crumpled and smooth states,  $\hat{\gamma} < 1$  and  $\hat{\gamma} > 1$ , respectively. The data collapse onto a single universal curve in each state. In the weak-swelling state (Fig. 4A) the mean area scales as  $\langle A \rangle = N f^<(\hat{\gamma})$ , whereas in the strong-swelling state (Fig. 4B) it scales as  $\langle A \rangle = N^2 f^>(\hat{\gamma})$ . These results confirm the scaling laws predicted by the Flory argument and mean-field theory, albeit with different scaling functions. The discrepancy in Figure 4A between the simulation results and the mean-field expression stems from the different definitions of the ring area discussed in section 2. In the simulation we measure the actual algebraic area, which vanishes at  $\gamma = 0$ . The calculation,

however, considers only positive algebraic areas (cf. Eq. (1)) and, hence, yields a finite mean area at zero fugacity,  $\langle A(0) \rangle = N(\ln 2)/(2\pi)$ . When this value of  $\langle A(0) \rangle$  is subtracted from the mean-field result (dotted line in Fig. 4A), the agreement with the simulations is excellent, indicating that the mean-field theory does accurately capture the swelling for  $\gamma < \gamma_c$ . On the other hand, the disagreement between simulation and theory in Figure 4B arises from the inadequacy of the mean-field approximation for stretched freely jointed chains, as was observed also in [14]. In Figure 4B we compare the data for a freely jointed chain subject to a pressure  $p > p_c$  [14] with those for fixed fugacity  $\gamma > \gamma_c$ . The two data sets are practically indistinguishable once one identifies  $p$  with  $\gamma$ .

Due to computation limitations we have not directly confirmed the asymptotic strong-swelling behavior at large  $\hat{\gamma}$  as given by equation (35); the equivalent asymptote for high pressure was confirmed in [14].

To test equation (8) for the cross-correlation of particle number and ring area we measured from the simulations the covariance  $C_{QA} = (\langle QA \rangle - \langle Q \rangle \langle A \rangle) / (\langle Q \rangle \langle A \rangle)$  for  $N = 50$  and varying  $\gamma$ . The results are presented in Figure 5 alongside the relative mean-square area fluctuations. The two data sets are indistinguishable, in agreement with equation (8). (In these measurements the area was taken as  $A_+$ .) As expected, the correlation is appreciable in the crumpled, unpressurized state (small  $\gamma$ ) and decays to zero as the ring swells into a smooth circle (large  $\gamma$ ).

## 5 Discussion

Fluctuating empty envelopes, such as the polymer rings studied previously [5, 6, 7, 8, 9, 10, 11, 12, 13, 14], have the special property that their thermodynamic state can be defined by specifying the surface degrees of freedom and intensive parameters only. For example, given the number of ring monomers  $N$ , temperature  $T$ , and pressure  $p$  of such an empty ring (actually,  $N$  and the ratio  $p/T$  suffice), one can completely characterize the system, including its extensive mean area  $\langle A \rangle$ . This situation is somewhat similar to the one encountered in the thermodynamics of electrodynamic modes in a cavity. Since the number of photons is unconstrained, the system can be defined without specifying an extensive parameter; given the surface properties of the cavity and the radiation pressure, one can determine the cavity volume.

In the current work the rings are not empty but enclose a gas of particles. Yet, we do not constrain their area, neither directly nor via a conjugate pressure. Hence, these systems still belong to the special category just described. When the number  $Q$  of trapped particles is prescribed, we find that the critical behaviors, previously reported for pressurized rings, disappear. The mechanism is qualitatively different from ordinary ones, where criticality is removed by disorder or fluctuations. It lies here in the absence of an area constraint, *i.e.*, in the freedom of these systems to select their mean area so as to maximize the total entropy. For a Gaussian ring we have found that the mean area is  $\langle A \rangle = NQ/(4\pi)$ , implying that the particles

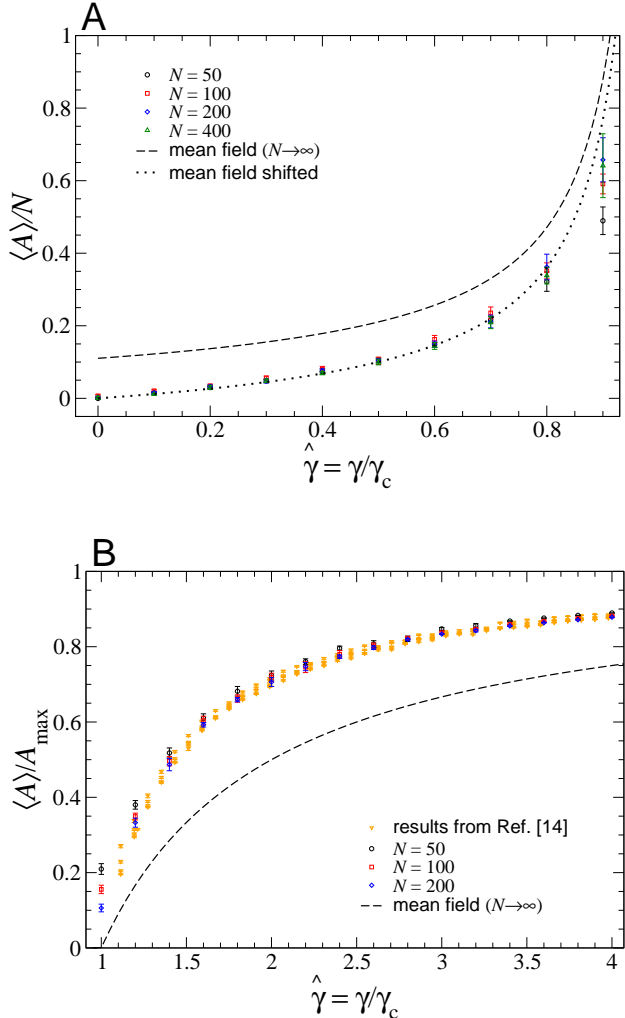


**Fig. 4.** (Color online) Mean area of a freely jointed ring as a function of particle fugacity below (A) and above (B) the critical point. The fugacity is scaled by  $\gamma_c = 4\pi/N$ , and the area by  $N$  in (A) and by  $A_{\max} = N^2/(4\pi)$  in (B). Symbols with error bars show the results of grand-canonical Monte Carlo simulations for different values of ring sizes  $N$ . The dashed lines show the mean-field prediction in the limit  $N \rightarrow \infty$ . The dotted line in (A) presents the mean-field result shifted down by  $\langle A(0) \rangle / N = (\ln 2)/(2\pi)$ . Panel (B) shows also simulation results from [14] for the swelling of a freely jointed ring with pressure  $p$ , for which the horizontal axis represents  $\hat{p} = p/p_c$ .

exert an effective pressure just equal to  $p_c = 4\pi/N$  for any  $Q > 0$ . The area never diverges, as it does for fixed  $p$ , but grows gradually, indefinitely, with increasing  $Q$ . For a freely jointed ring, by contrast, the mean area is such that the exerted pressure remains above  $p_c$  for any  $Q > 0$ . As a result, the swollen ring always obeys the smooth-state scaling law,  $\langle A \rangle \sim N^2 f(Q/N)$ .

When the particle fugacity  $\gamma$  is prescribed, the criticality of the two models is retained. In this case the system does not have the freedom to select the pressure exerted on its boundary, since  $p$  is determined by  $\gamma$  through the equation of state of the gas ( $p = \gamma$  for an ideal gas). The mod-

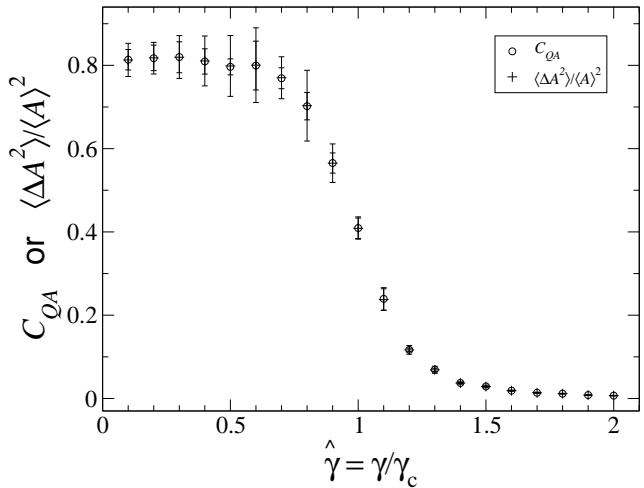


**Fig. 5.** Correlation between particle number and ring area as a function of particle fugacity, compared to the relative mean-square area fluctuations. Simulations were performed for an  $N = 50$  ring, and the ring area was taken as  $A_+$ .

els then become analogous to the fixed-pressure ones, as studied in [9, 14]. Thus, the canonical and grand-canonical ensembles are inequivalent in these systems. A vivid example is seen in the Gaussian model, where the canonical mean fugacity  $\gamma$  is found to be independent of  $Q$  (Eq. (14)), whereas the grand-canonical mean particle number does vary with  $\gamma$  (Eqs. (5) and (16)) and even diverges at  $\gamma_c$ . The former result of a fugacity independent of particle number is clearly a consequence of the unconstrained area. We infer, therefore, that this unusual property also underlies the ensemble inequivalence.

In the grand-canonical case we have derived, and confirmed in simulations, an identity relating the correlation between particle number and ring area with the area fluctuations (Eq. (8) and Fig. 5). The only assumption entering this derivation is the consideration of the particles as an ideal gas. Thus, the same identity should hold for any fluctuating envelope with unconstrained volume, enclosing an ideal gas of particles.

This study has been restricted to self-intersecting rings. When a self-avoidance term is added to the Flory grand potential of section 4.2.1, the second-order transition disappears, as in the case of fixed pressure [14]. We note, however, that the Flory argument does not reproduce the correct scaling regimes for pressurized self-avoiding rings as derived in [6, 7, 8].

The pressurized 2D envelopes studied here and in [14] are evidently idealized systems. Possible implications for more realistic systems of unconstrained volume, *e.g.*, 3D self-avoiding vesicles [24] with pores or aquaporin channels, are currently under study.

## Appendix A

### Area probability distribution function of a highly swollen freely jointed ring

Unlike the probability distribution function of the area for a Gaussian ring,  $P_0^G(N, A)$  of equation (9), its counterpart for a freely jointed ring,  $P_0^{FJ}(N, A)$ , is not known analytically. The asymptote of  $P_0^{FJ}$  as  $A \rightarrow A_{\max}$ , nonetheless, can be calculated, which is the aim of this Appendix.

A configuration of the ring is defined by a set of  $N$  2D vectors specifying the monomer positions,  $\{\mathbf{r}_j\}_{j=0, \dots, N}$  with  $\mathbf{r}_0 = \mathbf{r}_N$  to make the chain closed. The partition function for a fixed area  $A$  is given by

$$\begin{aligned} Z^{FJ}(N, A) &= \int \prod_{j=1}^N d\mathbf{r}_j \delta(|\mathbf{r}_j - \mathbf{r}_{j-1}| - 1) \delta(A'[\{\mathbf{r}_j\}] - A) \\ &= \int dp \int \prod_{j=1}^N d\mathbf{r}_j e^{ip(A'[\{\mathbf{r}_j\}] - A)} \delta(|\mathbf{r}_j - \mathbf{r}_{j-1}| - 1), \end{aligned} \quad (A.1)$$

where  $A'[\{\mathbf{r}_j\}]$  is the area of the configuration  $\{\mathbf{r}_j\}$ .

When the ring statistics is governed by highly swollen configurations, the integration over  $\{\mathbf{r}_j\}$  can be performed analytically using the transfer-matrix technique [14]. This leads to

$$Z^{FJ}(N, A \lesssim A_{\max}) = \int dp e^{-ipA} \left[ 2\pi I_0 \left( \frac{ipN}{4\pi} \right) \right]^N, \quad (A.2)$$

where  $I_0$  is the zeroth-order modified Bessel function of the first kind. The asymptotic expansion of  $I_0$  for large arguments,

$$I_0 \left( \frac{ipN}{4\pi} \right) \simeq \left( \frac{2}{ipN} \right)^{1/2} e^{\frac{ipN}{4\pi}}. \quad (A.3)$$

Substituting it in equation (A.2), we get, up to a constant prefactor,

$$Z^{FJ}(N, A \lesssim A_{\max}) \sim \int dp e^{ip(A_{\max} - A)} (pN)^{-N/2}, \quad (A.4)$$

which, upon a simple change of variables (or, alternatively, a stationary-phase approximation) readily yields

$$Z^{FJ}(N, A \lesssim A_{\max}) \sim (A_{\max} - A)^{N/2}. \quad (A.5)$$

Thus, the area probability distribution function, which is proportional to  $Z^{FJ}$ , is given to leading order in  $(A_{\max} - A)$  by

$$P_0^{FJ}(N, A \lesssim A_{\max}) \sim (A_{\max} - A)^{N/2}. \quad (A.6)$$

This result is used in section 4.1.3 to calculate the mean area of a freely jointed ring in the strong-swellling regime.

## References

1. M.G. Brereton, C. Butler, J. Phys. A **20**, 3955 (1987).
2. D.C. Khandekar, F.W. Wiegel, J. Phys. A **21**, L563 (1988); J. Phys. France **50**, 263 (1989).
3. B. Duplantier, J. Phys. A **22**, 3033 (1989).
4. B. Duplantier, Phys. Rev. Lett. **64**, 493 (1990).
5. J. Cardy, Phys. Rev. Lett. **72**, 1580 (1994).
6. S. Leibler, R.R.P. Singh, M.E. Fisher, Phys. Rev. Lett. **59**, 1989 (1987).
7. A.C. Maggs, S. Leibler, M.E. Fisher, C.J. Camacho, Phys. Rev. A **42**, 691 (1990).
8. C.J. Camacho, M.E. Fisher, Phys. Rev. Lett. **65**, 9 (1990).
9. J. Rudnick, G. Gaspari, Science **252**, 422 (1991).
10. G. Gaspari, J. Rudnick, A. Beldjenna, J. Phys. A **26**, 1 (1993).
11. E. Levinson, Phys. Rev. A **45**, 3629 (1992).
12. U.M.B. Marconi, A. Maritan, Phys. Rev. E **47**, 3795 (1993).
13. G. Gaspari, J. Rudnick, M. Fauver, J. Phys. A **26**, 15 (1993).
14. E. Haleva, H. Diamant, Eur. Phys. J. E **19**, 461 (2006).
15. R. Vilanove, F. Rondelez, Phys. Rev. Lett. **45**, 1502 (1980).
16. G.T. Gavranovic, J.M. Deutsch, G.G. Fuller, Macromolecules **38**, 6672 (2005).
17. B. Maier, J.O. Radler, Macromolecules **33**, 7185 (2000).
18. E. Ben-Naim, Z.A. Daya, P. Vorobieff, R.E. Ecke, Phys. Rev. Lett. **86**, 1414 (2001); R.E. Ecke, Z.A. Daya, M.K. Rivera, E. Ben-Naim, in *Materials Research Society Symposium Proceedings 759*, 2003, edited by S. Sen, M.L. Hunt, and A.J. Hurd (Warrendale, PA, 2003), p. 129.
19. M.B. Hastings, Z.A. Daya, E. Ben-Naim, R.E. Ecke, Phys. Rev. E **66**, 025102 (2002); Z.A. Daya, E. Ben-Naim, R.E. Ecke, e-print cond-mat/0603301.
20. M. Rubinstein, R.H. Colby *Polymer Physics* (Oxford University Press, Oxford, 2003).
21. R.A. Harris, J.E. Hearst, J. Chem. Phys. **44**, 2595 (1966); **46**, 398 (1967).
22. B.Y. Ha, D. Thirumalai, J. Chem. Phys. **103**, 9408 (1995); e-print cond-mat/9709345.
23. H. Diamant, D. Andelman, Phys. Rev. E **61**, 6740 (2000).
24. G. Gompper, D.M. Kroll, J. Phys. Condens. Matter **9**, 8795 (1997).